On the Impact of Prototype Filter Length on the PAPR Reduction of FBMC Signals

Brahim Elmaroud [#1], Ahmed Faqihi [#,*2], Mohammed Abbad [#3], Driss Aboutajdine [#4]

[#] LRIT, associated unit to CNRST (URAC-29), Faculty of Sciences,
Mohammed V-Agdal University Rabat, Morocco
[1] b.elmaroud@fsr.um5a.ma
[3] abbad@fsr.ac.ma
[4] aboutaj@fsr.ac.ma
[*] ENSIAS, Mohammed V-Souissi University Rabat, Morocco
[2] faqihi@ensias.ma

Abstract— One of the challenging issues for Filter Bank Multicarrier (FBMC) systems is their high Peak-to-Average Power Ratio (PAPR) which leads to the saturation of the high power amplifiers and consequently increases the out of band power. In this paper, we evaluate different FBMC PAPR reduction techniques and especially analyze the impact of the prototype filter length/overlapping factor on their performances.

Keyword- FBMC, prototype Filter Length, Peak-to-Average Power Ratio (PAPR), PAPR reduction techniques, Complementary Cumulative Distribution Function (CCDF).

I. INTRODUCTION

Filter Bank Multicarrier (FBMC) is a multicarrier modulation that consists of transmitting simultaneously N elementary symbols via N parallel orthogonal sub-channels. Although first introduced by Chang [1], Saltzberg [2] and Bellanger [3] in the mid 1960s/1970s, FBMC systems have just taken a special attention these last years, thanks to their advantages over conventional multicarrier modulation systems such as the famous Orthogonal Frequency Division Multiplexing (OFDM). Indeed, FBMC provides higher spectral efficiency than OFDM since it does not require a guard interval or cyclic prefix extension. Furthermore, orthogonality is required only for neighboring sub-channels due to the special Nyquist filter used in FBMC systems, which is characterized by its reduced out-of-band ripples and its high frequency selectivity [3]. For a detailed description of FBMC systems, the interested reader can refer to [3]-[7].

Unfortunately, since FBMC signal, like in any other multicarrier system, is the sum of a large number of independently modulated subcarriers, it suffers from high Peak-to-Average Power Ratio (PAPR). This leads nonlinear devices and especially Power Amplifiers to operate in their saturation region and thus impair system performance by adding significant spectral spreading and in-band distortion [8], [9]. To overcome this problem, many PAPR reduction approaches have been proposed. The most considerable are: Clipping [8], coding schemes [10], Hadamard transform [11], nonlinear companding transforms [12]-[14], Tone Reservation (TR) and Tone Injection (TI) [15], [16], Selected Mapping (SLM) [17]-[19] and Partial transmit Sequences (PTS) [20]-[22]. For FBMC systems clipping [23]-[25] and SLM method [26] have been used for PAPR Reduction. In [23], the effects of clipping on spectral regrowth and BER performance were highlighted. To limit the BER degradation, an efficient but complex iterative noise cancelation technique, called Bussgang noise cancelation, was applied at the receiver [24]. In [25], this last technique was compared with tone reservation, active constellation extension and their combination. In [26] a method called Overlapped SLM (OSLM) has been employed to reduce the PAPR of FBMC systems.

In this paper, we will firstly, analyze the performances of four PAPR reduction technique for FBMC signals; SLM method, Hadamard transform, exponential companding transform and the combination of Hadamard and a non linear companding transforms proposed for OFDM systems in [27] and adapted for FBMC systems in this work (using exponential compnading transform which is a special case of non linear companding transforms). Then, we will take into account the prototype filter length of the considered FBMC system to evaluate its impact on the presented PAPR reduction techniques. In other words, we aim to highlight the effect of the prototype filter length on the studied PAPR reduction techniques.

The remainder of this paper is organized as follows: In section II, the considered FBMC system model is presented. Section III is devoted to the high PAPR problem formulation and its distribution function. In section IV, the four studied PAPR reduction techniques are described. Section V reports simulation results, including the performance evaluation of the considered PAPR reduction techniques and the effect of the prototype filter length on thereof. Finally, conclusions are drawn in Section VI.

II. FBMC SYSTEM

Basically, a multicarrier system can be implemented using an Inverse Fast Fourier Transform (IFFT) as a modulator (transmitter), and a Fast Fourier Transform (FFT) as a demodulator (receiver). Therefore, the complex envelope of the transmitted multicarrier signal at the IFFT output can be expressed by [4]:

$$s_n(m) = \sum_{i=0}^{N-1} d_i(m) e^{j2\pi \frac{in}{N}}, \qquad 0 \le n \le N-1 \tag{1}$$

Where N is the number of subcarriers and $d_i,\ 0 \le i \le N-1$ are the elementary input symbols (BPSK, QPSKA… symbols).

At the receiver side, the data samples are recovered by:

$$d_i(m) = \frac{1}{N} \sum_{n=0}^{N-1} s_n(m) e^{-j2\pi \frac{in}{N}}, \qquad 0 \le i \le N-1 \tag{2}$$

However, in practice and in the presence of multipath channels, it is not possible to recover the transmitted symbols with a simple FFT because of the symbol overlapping and intercarrier interference introduced by the channel impulse response. To overcome this problem and maintain subcarriers orthogonality, OFDM systems add a guard time called cyclic prefixe (CP) to the symbol duration. FBMC systems on the other side, use a special Nyquist filter characterized by its reduced out-of-band ripples and its high frequency selectivity. This special filter is split into two parts, one part for the transmitter and the second for the receiver. Then, the bank of filters is constructed by frequency shifting N copies of the half-Nyquist filter (prototype filter).

A basic FBMC transmitter as described in [4] is shown in Figure 1. In this scheme, an elementary symbol modulates 2K-1 subcarriers (K is the prototype filter frequency response length or the overlapping factor). Accordingly, an iFFT of size KN is considered, and every elementary symbol $d_i,\ 0 \le i \le N-1$ is multiplied by the filter frequency coefficients according to the following expression:

$$ds = (d_0 H \quad d_1 H \quad \cdots \quad d_{N-1} H)^T \tag{3}$$

Where $H = [H_0 \quad H_0 \quad \cdots \quad H_{K-1}]^T$ are the K prototype filter frequency coefficients and x^T denotes the transpose of x.

The resulting symbols $ds_i,\ 0 \le i \le KN-1$ undergo an overlap operation to produce overlapped symbols given by:

$$ds_i^o = \sum_{k=i-(K+1)}^{i+(K-1)} ds_i, \qquad i = K+1, \cdots, K(N-1) \tag{4}$$

This means that every ds_i symbol is fed to 2K − 1 inputs of the iFFT ($i-(K+1)$ to $i+(K-1)$). Such processing is called ”weighted frequency spreading” (WFS) because each elementary symbol is spread over several iFFT inputs.

Finally, the signal at the output of the iFFT becomes:

$$s_n(m) = \sum_{i=0}^{KN-1} ds_i^o(m) e^{j2\pi \frac{in}{KN}}, \qquad 0 \le n \le KN-1 \tag{5}$$

At the receiver, the inverse operations are applied and the elementary symbols are recovered by the weighted frequency despreading (WFDs) operation resting on the following property:

$$\frac{1}{N} \sum_{k=-(K-1)}^{(K-1)} |H_k|^2 = 1 \tag{6}$$

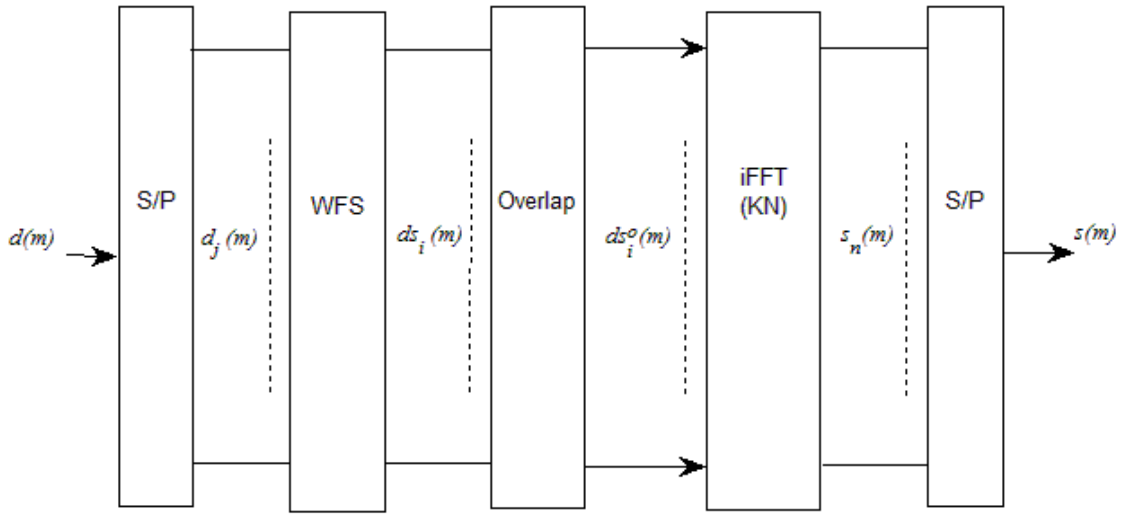

Fig. 1. Filter Bank Multicarrier transmitter

It is clear that the presented FBMC system provides a notable improvement over the conventional IFFT scheme. Nevertheless, one can notice the significant redundancy added due to the overlapping of the IFFT/FFT outputs/inputs. This redundancy is accompanied with an increase in the size of the IFFT/FFT leading to an increase in the computation complexity. An efficient approach to reduce this complexity and keep the IFFT size to N can be applied and is called "Polyphase Network" (PPN). A detailed description of the PPN-Implementation can be found in [3], [4].

III. PAPR PROBLEM FORMULATION AND CCDF

The Peak-to-Average Power Ratio of a given signal s(t) is defined as the ratio of the peak power of s(t) to its average power. The PAPR is a parameter that measures the sensitivity to nonlinear devices of transmission schemes having non-constant envelope and especially multicarrier modulations.

The PAPR of the complex envelope s(t) of a continuous baseband signal transmitting complex symbols with duration can be written as [9], [28]:

$$PAPR(s(t)) = \frac{\max_{[0,T_0]} |s(t)|^2}{\frac{1}{T_0}\int_0^{T_0} |s(t)|^2 dt} \tag{7}$$

If we consider a discrete time signal and especially an FBMC signal with N sub-carriers, the PAPR is defined by [26]:

$$PAPR(s[n]) = \frac{\max_{0\le n<N} |s[n]|^2}{E\left[|s[n]|^2\right]} \tag{8}$$

For FBMC signals, the cumulative distribution function (CDF) of the PAPR which gives the probability that the PAPR is below some threshold level γ can be written as [9], [28]:

$$CDF(\gamma) = \Pr(PAPR(s[n]) \le \gamma) = \left(1 - e^{-\gamma}\right)^N \tag{9}$$

Therefore, the complementary cumulative distribution function (CCDF) of PAPR which provides the probability that the PAPR is above some threshold level γ is given by:

$$CCDF(\gamma) = \Pr(PAPR(s[n]) > \gamma) = 1 - \left(1 - e^{-\gamma}\right)^N \tag{10}$$

IV. PAPR REDUCTION TECHNIQUES FOR FBMC SYSTEMS

A. *Selected Mapping method (SLM)*

SLM is a distortion-less PAPR reduction technique first described by Bauml et al [17]. The block diagram of the SLM-FBMC transmitter is shown in Figure 2. In this scheme U different versions of the same multicarrier

(FBMC in our case) symbol are generated by multiplication of the bloc of KN modulated data symbols ds_i^o, $0 \le i \le KN-1$ with a set of U distinct pseudo-random vectors of length KN denoted by $P^{(u)}$, $1 \le u \le U$. Each vector $P^{(u)}$ is expressed by:

$$P^{(u)} = \left[P_0^{(u)}, \cdots, P_{KN-1}^{(u)}\right] \tag{11}$$

Where $P_i^{(u)} = e^{j\varphi_i^u}$, $\varphi_i^u \in [0, 2\pi]$.

The set of the U independent FBMC symbols so obtained can be expressed by:

$$ds_i^{oSLM\ (u)} = ds_i^o P_i^{(u)},\ 1 \le u \le U\ \&\ 0 \le i \le KN-1 \tag{12}$$

Finally, the U FBMC symbols are transformed to time domain (via iFFT) to obtain U versions of the transmitted signal s_n and the signal version with the lowest PAPR is selected for transmission.

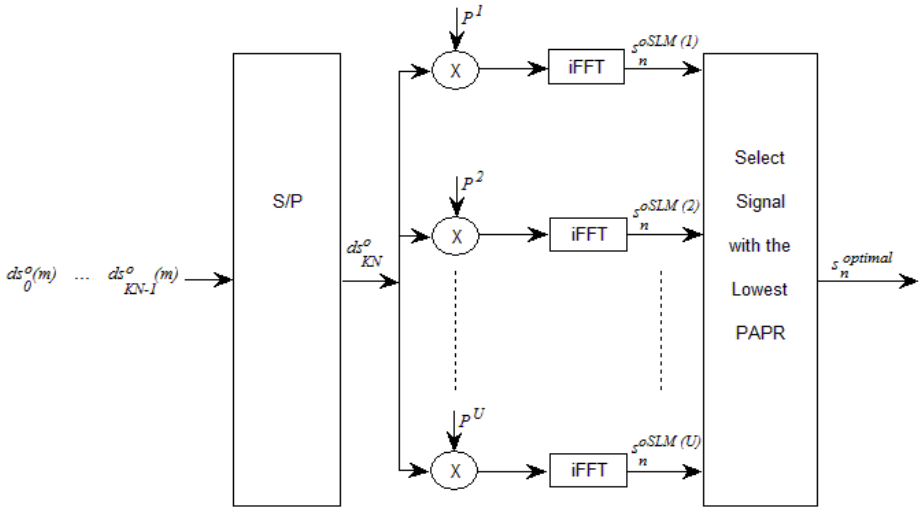

Fig.2. Block diagram of SLM-FBMC transmitter

B. Exponential Companding transform

Non-linear companding transforms are a set of efficient PAPR reduction techniques designed for multicarrier signals and characterized by their good system performance and low implementation complexity. In particular, the Exponential companding transform provides improved system performances in terms of PAPR reduction, BER, power spectrum and phase error [14]. In this scheme, FBMC symbols s_n are companded using an exponential companding function and then transmitted through the channel. The companded signal t_n is given by:

$$t_n = h(s_n) \tag{13}$$

Where h(.) is the exponential companding function which is expressed by [14]:

$$h(x) = \mathrm{sgn}(x)\sqrt[d]{\alpha\left[1 - \exp\left(-\frac{x^2}{\sigma^2}\right)\right]} \tag{14}$$

Where, Sgn(.) is the sign function, d is the degree of the exponential companding, σ^2 is the signal variance and α is a positive constant which determines the average power of input signal [14]:

$$\alpha = \left(\frac{2\sigma^2}{E\left[\sqrt[d]{\left[1 - \exp\left(-\frac{x^2}{\sigma^2} \right) \right]^2} \right]} \right)^{\frac{d}{2}} \tag{15}$$

At the receiver, the expanding operation is applied using the inverse function of h denoted by h^{-1} and expressed by:

$$h^{-1}(x) = \mathrm{sgn}(x) \sqrt{-\sigma^2 \log_e \left(1 - \frac{x^d}{\alpha} \right)} \tag{16}$$

C. Hadamard transform

Hadamard transform is a simple technique [11] which proposes to transform the KN sequence ds_i^o, $0 \le i \le KN-1$ using KN order Hadamard matrix H_{KN}. Therefore, a multiplication by the inverse of H_{KN} denoted by H_{KN}^{-1} is required at the receiver to recover the transmitted sequence.

Hadamard matrix can be simply generated by recursive procedure [29]:

$$H_2 = \frac{1}{\sqrt{2}} \begin{pmatrix} 1 & 1 \\ 1 & -1 \end{pmatrix}, \; H_{2N} = \frac{1}{\sqrt{2N}} \begin{pmatrix} H_N & H_N \\ H_N & H_N^{-1} \end{pmatrix} \tag{17}$$

Mathematically, Hadamard transform can be summarized as follows:

$$\hat{ds}_{KN} = H_{KN}^{-1} \left(FFT\left\{ IFFT\left\{ H_{KN} ds_{KN}^o \right\} + n \right\} \right) \tag{18}$$

Where $ds_{KN}^o = ds_0^o, \cdots, ds_{KN-1}^o$ represents the transmitted FBMC symbol and $\hat{ds}_{KN}$ the received one corrupted by the noise vector n.

D. Combining exponential companding and Hadamard transforms

To improve the PAPR reduction of OFDM signals, [27] has proposed to combine Hadamard transform with a non linear companding transform. In this section, we present an adaptation of this combination to FBMC systems using exponential companding transform. The weighted frequency spread and overlapped symbols ds_{KN}^o are first transformed by Hadamard matrix H_{KN}, then the resulting symbols are fed to the KN iFFT inputs. Finally, the exponential companding transform takes place and the companded FBMC signal is transmitted. At the receiver, the inverse operations are applied in the appropriate order as shown in figure 3.

The proposed processing is described as follows [27]:

- **Step 1**: The weighted frequency spread and overlapped symbols ds_{KN}^o are transformed by Hadamard matrix H_{KN} : $D_{KN} = H_{KN} ds_{KN}^o$
- **Step 2**: The transformed symbols are fed to the iFFT inputs: $s_{KN} = IFFT(D_{KN})$
- **Step 3**: The exponential companding takes place : $t_{KN} = h(s_{KN})$
- **Step 4**: The inverse exponential companding is applied at the receiver[1]: $\hat{s}_{KN} = h^{-1}(r_{KN})$
- **Step 5**: $\hat{s}_{KN}$ is transformed to frequency domain (FFT): $\hat{D}_{KN} = FFT(\hat{s}_{KN})$
- **Step 6**: Inverse Hadamard transform is applied to $\hat{D}_{KN}$: $\hat{d}_{KN} = H_{KN}^{-1} \hat{D}_{KN}$

[1] $r_{KN} = t_{KN} + noise$

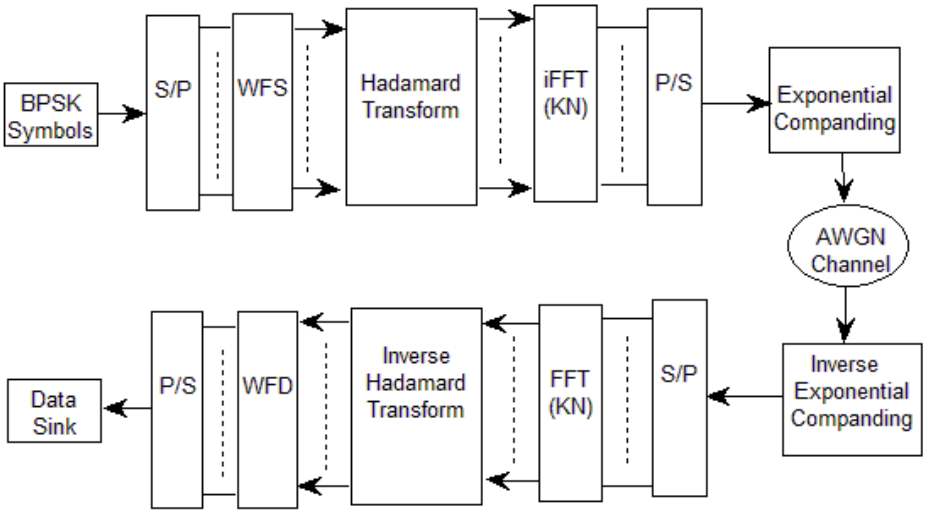

Fig. 3. Block diagram of a baseband FBMC system with the Hadamard-exponential companding combined PAPR reduction scheme.

V. Simulation Results

This section is divided into two subsections. The first subsection presents performance evaluation of the simulated PAPR reduction techniques for the basic FBMC system introduced in section II. In the second subsection, we evaluate the impact of the prototype filter length on the performance of each PAPR reduction technique separately.

In all our simulations, the transmitted real data d_k, $0 \le k \le N-1$ are derived from a BPSK modulation and we keep the same number of sub-channels N = 64. Regarding the FBMC system, Phydyas [4] prototype filter is used, and coefficients presented in [30] are applied. In addition, we have chosen an additive White Gaussian Noise (AWGN) channel. Table I shows the summary of the simulation parameters for the considered FBMC modulation system. Note that the overlapping factor K is fixed at the value 4 in subsection V-A. Nevertheless, this important parameter has a significant influence on the PAPR reduction techniques performance. This is why in subsection V-B, we have considered different values of K (1, 2, 4 and 8) in order to evaluate its impact on the simulated PAPR reductions techniques.

TABLE I
Simulation parameters for the considered FBMC system

Parameter		Value
Bandwidth		1 MHz
Number of sub-channels N		64
Overlapping factor K	Subsection V-A	4
	Subsection V-B	1, 2, 4, and 8
Number of subcarriers nFFT		nFFT=KN
Mapping		BPSK

For SLM scheme, the rotation factors belong to the set {+1, −1, +j, −j} and the number of possible phase factor combinations is $4^N = 4^{64}$. From all these combinations, U=8 vectors are chosen to obtain the 8 independent FBMC symbols given in (12). The exponential Companding transform is based on [14] and Hadamard matrix of length 64 has been employed for Hadamard transform. Finally, the combination of these two latter methods is based on section IV-D.

A. *Performance evaluation of the simulated PAPR reduction techniques*

This section presents performance evaluation of the simulated PAPR reduction techniques for the basic FBMC scheme described in section II.

Figure 4 shows different plots of the CCDF-PAPR curves for 10^3 randomly generated FBMC symbols and different PAPR reduction schemes. A Hadamard-exponential companded OFDM signal has been also

considered for comparison purposes. From Figure 4, it is very clear that the Hadamard-exponential companding combined scheme provides the best PAPR reduction performance compared with the SLM method, Hadamard transform and exponential companding transform. For example, when $CCDF = 10^{-2}$, the combined scheme reduces the PAPR by 5.1 dB, 3.9 dB and 2.2 dB over Hadamard transform, SLM method and exponential companding transform respectively. Nevertheless, it is worth noting that the SLM method can improve its PAPR reduction performance and approach those of the exponential companding transform by increasing the number of chosen vectors U; however, this will also increase computational complexity.

Table II depicts, for $CCDF = 10^{-2}$, the PAPR values of the original FBMC signal and the FBMC signal after applying the studied PAPR reduction techniques. As we can see, the Hadamard-exponential companded OFDM signal shows a slightly lower PAPR than the FBMC one (4 dB for OFDM against 4.1 dB for FBMC, when $CCDF = 10^{-2}$). Nevertheless, one should notice that the FBMC system considered in this work is a basic version of the complex and optimal FBMC system with Polyphase implementation [4]. In fact, in the optimal FBMC system, the PAPR is lower [24]-[26] and the studied PAPR reduction techniques could offer better results.

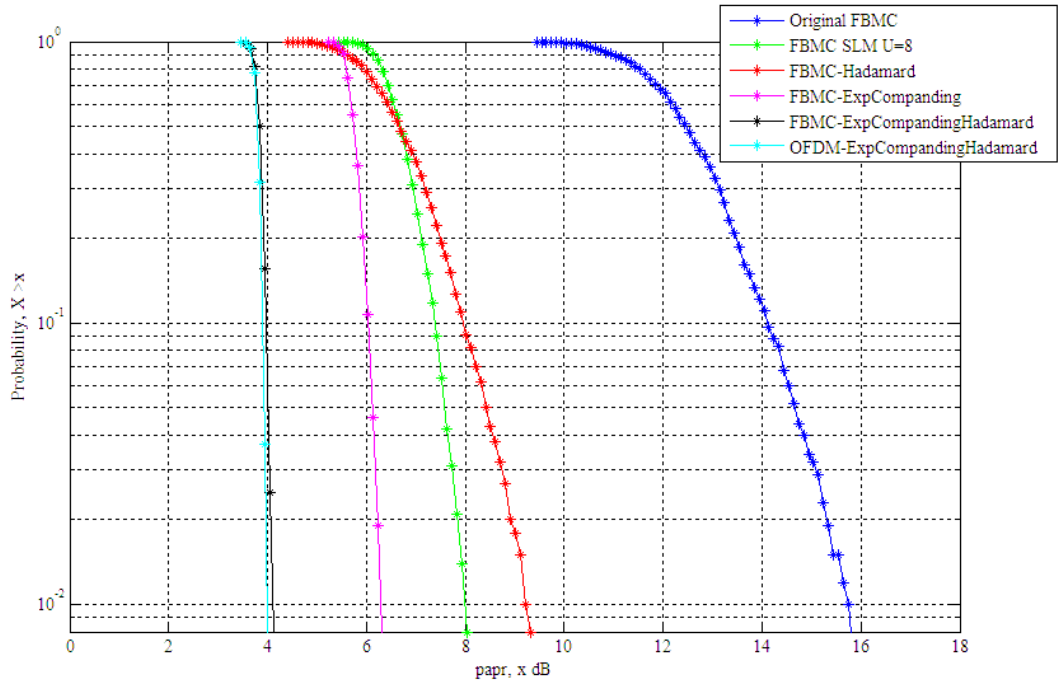

Fig. 4. CCDF-PAPR comparison for the simulated FBMC systems

TABLE III

PAPR values corresponding to $CCDF = 10^{-2}$ for the simulated PAPR reduction schemes

Signal	PAPR value in
Original FBMC signal	15.7
FBMC-Hadamard transform	9.2
FBMC-SLM method	8
FBMC-Exponential companding transform	6.3
FBMC-Hadamard and exponential companding transforms	4.1
OFDM-Hadamard and exponential companding transforms	4

B. *Effect of the prototype filter length on the PAPR reduction of FBMC signals*

As above mentioned, the prototype filter length K has a significant influence on the PAPR distribution of FBMC signals. In order to evaluate this influence, we have considered four prototype filter lengths K=1, 2, 4 and 8. As shown in Figure 5, different curves of the CCDF have been given for different PAPR reduction schemes and for various prototype filter lengths. In addition, Table III shows, for $CCDF = 10^{-2}$, the PAPR values of the considered FBMC signals depending on the prototype filter length K.

It is clear from Figure 5 and Table III that the parameter K has an important impact on the PAPR distribution. Hence, the PAPR increases for large values of K. In other words, the PAPR increases when the symbols overlap

becomes significant. On the other side, with short Phydyas prototype filter lengths, the PAPR decreases. This holds true for all the simulated PAPR reduction techniques with some differences. Indeed, the impact of varying K is significant for SLM method and exponential companding transform. For Hadamrad transform and the combined scheme, the influence is, respectively, medium and minor (except for K=1).

To ensure that the obtained experimental results match with the theory, we carry on a quick theoretical analysis in which we consider the expression of PAPR of an FBMC signal presented in (8). Considering the FBMC system showed in Figure 1, (8) may be written as:

$$PAPR(s_n) = \frac{\max_{0 \le n < KN} |s_n|^2}{E\left[|s_n|^2\right]} \tag{19}$$

With:

$$E\left[|s_n|^2\right] = \sum_{n=0}^{KN-1} \frac{|s_n|^2}{KN} \tag{20}$$

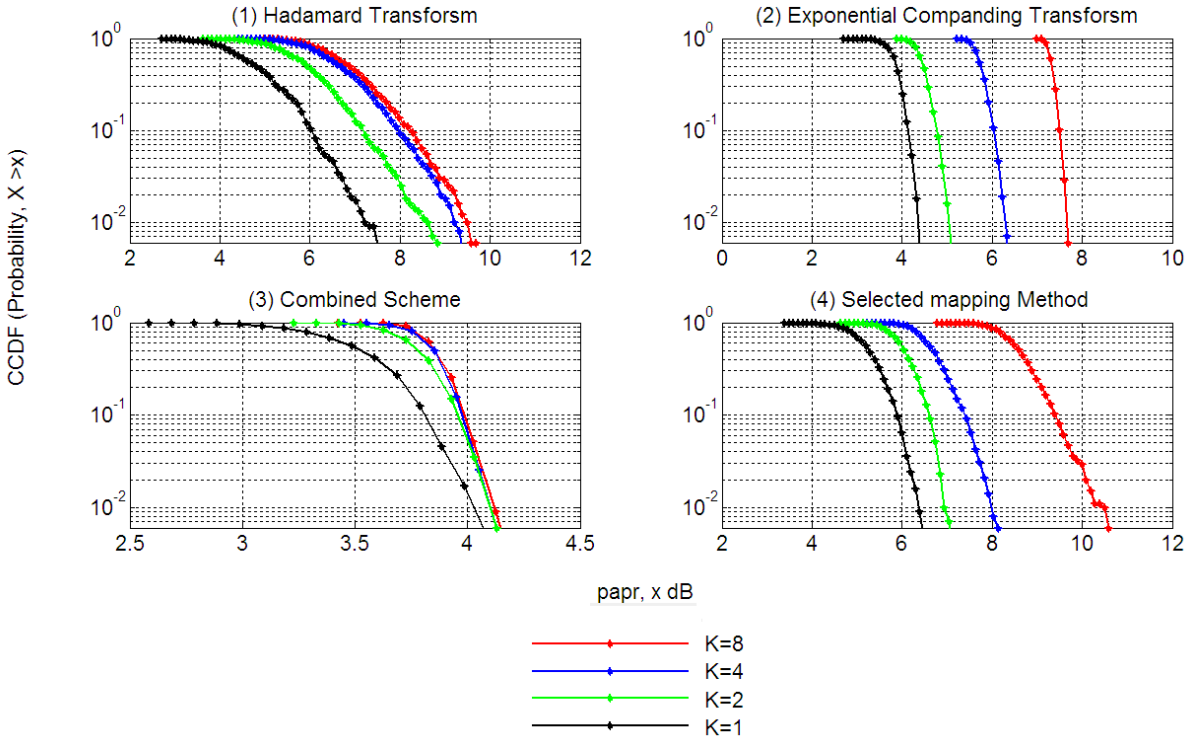

Fig. 5. CCDF-PAPR for different PAPR reduction schemes and for various prototype filter lengths

Let $s_{2\max} = \max_{0 \le n < KN} |s_n|^2$ Then, it follows from (20) that (19) can be rewritten as:

$$PAPR(s_n) = KN \frac{s_{2\max}}{\sum_{n=0}^{KN-1} |s_n|^2} \tag{21}$$

On the other hand, if we assume that the input symbols $d_i[m],\ 0 \le i \le N-1$ are independent and identically distributed (iid), then, it follows from the central limit theorem that, for large values of N, the real and imaginary parts of $d_i[m],\ 0 \le i \le N-1$ are iid Gaussian random variables, and thus, we can express the CCDF using (10) [9],[28]. For the FBMC system considered in this work, the number of subcarriers is KN instead of N. In this case, the equation (10) should be written as follows:

$$CCDF(\gamma) = 1 - \left(1 - e^{-\gamma}\right)^{KN} \tag{22}$$

TABLE III

PAPR values corresponding to $CCDF = 10^{-2}$ for the simulated PAPR reduction schemes and for different values of K

PAPR Reduction Scheme	Prototype Filter Length K	PAPR value in dB
Hadamard transform	1	7.2
	2	8.6
	4	9.2
	8	9.5
Exponential companding transform	1	4.3
	2	5
	4	6.3
	8	7.7
Exponential companding and Hadamard transforms combined	1	4.03
	2	4.09
	4	4.10
	8	4.12
Selected mapping method	1	6.4
	2	6.9
	4	8
	8	10.5

From (21) and (22), it is straightforward to report that the PAPR increases when the prototype filter length K increases. This matches with the experimental results presented in this section. Indeed, we have shown for all the simulated techniques that the PAPR reduction performance decreases when K increases. Therefore, from all these results, one can conclude that short prototype filter length is more advantageous and the ideal choice is K=1 thanks to the lower PAPR provided and the minimum computational complexity and storage requirements. Nevertheless, we should not ignore that one of the main advantages of FBMC systems is the symbols overlap, thus, the FBMC system performance raises as the overlapping factor K increases. So it is required, when choosing K, to find a trade-off between reducing the PAPR and holding the advantages of FBMC systems.

VI. CONCLUSION

In this paper, a basic FBMC system was presented and various PAPR reduction techniques were applied and evaluated. In order to assess the impact of the prototype filter length K on the performance of the studied PAPR reduction techniques, different lengths of the Phydyas prototype filter have been considered. Simulation results have confirmed that as K increases the PAPR reduction performance decreases for all the simulated techniques. It was concluded that a trade-off between PAPR reduction and FBMC system performance should be found. This work can be extended by considering a complex FBMC system with Polyphase implementation.

ACKNOWLEDGMENT

The authors are grateful to Maurice Bellanger (CNAM, Paris) and Zakaria Mohammadi (LRIT, FSR Rabat) for fruitful discussions.

REFERENCES

[1] R. W. Chang, “High-speed multichannel data transmission with bandlimited orthogonal signals”, Bell Syst. Tech. J., vol. 45, Dec. 1966, pp. 1775–1796.
[2] B. R. Saltzberg, “Performance of an efficient parallel data transmission system”, IEEE Trans. Commun. Tech., vol. 15, no. 6, Dec. 1967, pp. 805–811.
[3] M. Bellanger and J. Daguet, “TDM-FDM transmultiplexer: Digital polyphase and FFT”, IEEE Trans. Commun., vol. 22, no. 9, Sept. 1974, pp. 1199–1205.
[4] M. Bellanger, “FBMC physical layer: a primer”, PHYDYAS project. http://www.ict-phydyas.org/
[5] P. Siohan, C. Siclet, and N. Lacaille, “Analysis and design of OFDM-OQAM systems based on filterbank theory,” IEEE Trans. Signal Processing, vol. 50, no. 5, May 2002, pp. 1170–1183.
[6] B. Farhang-Boroujeny and C. H. G. Yuen, “Cosine modulated and offset QAM filter bank multicarrier techniques: A continuous-time prospect”, EURASIP J. Adv. Signal Processing [Online]. vol. 2010, 16 p, DOI: 10.1155/2010/165654.
[7] B. Farhang-Boroujeny, “OFDM versus filter bank multicarrier”, IEEE Signal Process. Mag., vol. 28, no. 3, 2011, pp.92 -112.
[8] R. O. Neill and L. B. Lopes, “Envelope variations and spectral splatter in clipped multicarrier signals”, in Proc. IEEE Int. Symp. Personal, Indoor Mobile Radio Commun., Toronto, ON, Canada, Sep. 1995, pp. 71-75.
[9] H. Ochiai and H. Imai, ”On the distribution of the peak-to-average power ratio in OFDM signals”, IEEE Trans. on Communications, vol. 49, no. 2, 2001, pp.282 -289.
[10] A. E. Jones, T. A.Wilkinson, and S. K. Barton, “Block coding scheme for reduction of peak to mean envelope power ratio of multicarrier transmission schemes”, IEEE Electronics Letters, vol. 30, no. 8, Dec. 1994, pp. 20982099.
[11] Myonghee Park, Heeyoung Jun, Jaehee Cho, Daesik Hong, Changuen Kang, ”PAPR reduction in OFDM transmission using Hadamard transforms,” IEEE International Conference on Communications, New Orleans, LA, June 2000, pp. 430-433.
[12] X. B.Wang, T. T. Tjhung, and C. S. Ng, “Reduction of peak-to-average power ratio of OFDM system using a companding technique”, IEEE Trans. Broadcasting, vol. 45, no. 3, Sept. 1999, pp. 303-307.

[13] X. Huang, J. H. Lu, J. L. Zheng, K. B. Letaief, and J. Gu, “Companding transform for reduction in peak-to-average power ratio of OFDM signals”, IEEE Trans.Wireless Communications, vol. 3, no. 6, Nov. 2004, pp. 2030-2039.
[14] T. Jiang, Y. Yang, and Y. Song, “Exponential companding transform for PAPR reduction in OFDM systems,” IEEE Trans. Broadcasting, vol. 51, no. 2, Jun. 2005, pp. 244–248.
[15] S. S. Yoo, S. Yoon, S. Y. Kim, and I. Song, “A novel PAPR reduction scheme for OFDM systems: Selective mapping of partial tones (SMOPT)”, IEEE Trans. Consumer Electronics, vol. 52, no. 1, Feb. 2006, pp. 40-43.
[16] J. Tellado, “Peak to Average Power Ratio Reduction for Multicarrier Modulation”, PhD thesis, University of Stanford, Stanford, 1999.
[17] R. W. Bauml, R. F. H. Fisher, and J. B. Huber, “Reducing the Peak-to-Average Power Ratio of Multicarrier Modulation by Selected Mapping,” IEEE Electronics Letters, vol. 32, no. 22, Oct. 1996, pp. 2056–2057.
[18] S. Goff , B. Khoo , C. Tsimenidis and B. Sharif, ”A novel selected mapping technique for PAPR reduction in OFDM systems”, IEEE Trans. Communications, vol. 56, no. 11, 2008, pp.1775 -1779.
[19] M. F. Naeiny and F. Marvasti, ”Selected Mapping algorithm for PAPR reduction of space frequency coded OFDM systems without side information”, IEEE Trans. Veh. Technol., vol. 60, no. 3, 2011, pp.1211 -1216.
[20] S. H. Muller and J. B. Huber, “OFDM with reduced peak-to-average power ratio by optimum combination of partial transmit sequences”, IEEE Electronics Letters, vol. 33, no. 5, Feb. 1997, pp. 368-369.
[21] S. H. Muller and J. B. Huber, ”A comparison of peak power reduction schemes for OFDM”, Proc. of GLOBECOM´97, Phoenix, AZ, vol. 1, 1997, pp.1-5.
[22] L. J. Cimini and N. R. Sollenberger, ”Peak-to-average power ratio reduction of an OFDM signal using partial transmit sequences”, IEEE Commun. Lett., vol. 4, no. 3, 2000, pp.86 -88.
[23] M. U. Rahim, T. H. Stitz, and M. Renfors, “Analysis of clipping-based PAPR reduction in multicarrier systems”, in the proceedings of IEEE VTC Spring 2009, Barcelona, April 2009, pp. 1-5.
[24] Z. Kollar and P. Horvath, “PAPR reduction of FBMC by clipping and its iterative compensation”, Journal of Computer Networks and Communications, vol. 1, no. 1, Feb. 2012, 11 pages.
[25] Z. Kollar, L. Varga, and K. Czimer, “Clipping-based iterative PAPR reduction techniques for FBMC”, in the proceeding of InOWo, Essen, Germany, Aug. 2012, pp. 1-7.
[26] A. Skrzypczak, J. Javaudin, and P. Siohan, “Reduction of the peak-to- average power ratio for the OFDM/OQAM modulation”, in the proceeding of IEEE VTC, Melbourne, Australia, May 2006, pp. 2018-2022.
[27] Z. Wang, S. Zhang and B. Qiu, “PAPR reduction of OFDM signal by using Hadamard transform in companding techniques”, 12th IEEE International Conference on Communication Technology (ICCT), Nanjing, November 2010, pp. 320-323.
[28] R. Prasad, “OFDM for Wireless Communications Systems”, Artech House, Norwood, MA, 2004, pp. 149–152.
[29] K. R. Rao and N. Ahmed, "Orthogonal transforms for digital signal processing," IEEE International Conference on Acoustics, Speech, and Signal Processing, vol. 1, 1976, pp. 136-140.
[30] S. Mirabbasi and K. Martin, “Design of prototype filter for near-perfect reconstruction overlapped complex-modulated transmultiplexers,” in Proc. IEEE International Symposium on Circuits and Systems (ISCAS), Phoenix-Scottsdale, AZ, vol. 1, 2002, pp. 821–824.